Wind and Structures, Vol. 12, No. 2 (2009) 133-149
DOI: http://dx.doi.org/10.12989/was.2009.12.2.133

The physical simulation of thunderstorm downbursts using an impinging jet

McConville A. C.

Arup, 13 Fitzroy Street, London, UK

Sterling M.* and Baker C. J.

School of Civil Engineering, The University of Birmingham, Edgbaston, Birmingham, B15 2TT, UK

(Received June 5, 2008, Accepted January 16, 2009)

Abstract. This paper outlines the results of a physical simulation (at a 1:700 - 1:1000 geometric scale) of a thunderstorm downburst. Three different methods are examined in order to generate the time dependent nature of a downburst: directly controlling the fans and via two different types of opening apertures. Similarities are shown to exist between each method, although the results obtained from one approach are favoured since they appear to be independent of the downdraft velocity. Significant run-to-run variations between each experiment are discovered and in general it is found beneficial to interpret the results in terms of 10 run ensemble averages. An attempt to simulate a translating downburst is also undertaken and the results are shown to compare favourably with full-scale data.

Keywords: thunderstorms; downburst; impinging jet; transient simulations.

1. Introduction

The last few years has witnessed a renewed interest in the effects of non-synoptic winds. For example, Durañona, *et al.* (2006) examined the structure of extreme gusts corresponding to a variety of non-synoptic winds and discovered that the streamwise velocity profile can differ significantly from that of a 'typical' gust associated with boundary layer winds. Recently attention has been focused on the simulation of a thunderstorm downburst. In addition to being scientifically interesting, these winds have practical importance, since in many areas of the world they are responsible for the design wind speed. Such downbursts have been described by a number of authors (Byers 1959; Wakimoto 1982; Wakimoto 2001; Lin and Savory 2006) with perhaps the two most notable being the Andrews Air Force Base downburst of 1983 (Fujita 1985) and the Lubbock-Reese rear-flank downdraft of 2002 (Holmes, *et al.* 2008). However, for the purpose of this paper it is sufficient to acknowledge that a thunderstorm can give rise to a downwards movement of air, i.e. a 'downdraft', and in some cases this flow impinges on the ground causing the resultant air to be displaced radially outwards from the point of impingement. As a result, a ring vortex travels away from the stagnation

* Corresponding Author, E-mail: m.sterling@bham.ac.uk

point causing the mean streamwise velocity profile and corresponding gust profile to differ significantly from that associated with normal atmospheric boundary layer winds. Recently, there have been a number of attempts to simulate physically wind characteristics which can be attributed to downbursts. This work is briefly discussed in Section 2 of the paper. Section 3 describes the design of the large scale Birmingham downdraft simulator and, using this facility, the effect that different gust generating devices can have on the downburst is examined (Section 4). Section 5 considers the issues associated with the scaling of physically simulated downburst, and undertakes a comparison with full-scale data from the Andrews Air Force Base event. Conclusions are drawn in Section 6.

2. Physical Modelling

2.1. Impinging jets

There has been a variety of physical experiments examining the flow dynamics of an impinging jet. Walker (1992) and Letchford, *et al*. (2002) were perhaps the first to articulate formally the need for such experiments to be examined from a wind engineering perspective, although it is acknowledged that others had previously undertaken work in this area (e.g. Holmes 1992; Wood, *et al.* 2001). It could be argued that Letchford is perhaps responsible for advancing this subject the most in terms of physical simulations. In his early work (Letchford and Chay 2002; Chay and Letchford 2002) a 'moving jet wind tunnel' was used, which was essentially a centrifugal blower capable of translational movement. Later experiments undertaken by Mason, *et al*. (2005) removed the effect of transient motion and focused on generating a 'pulsed' downdraft. These experiments involved the application of a novel aperture in order to generate pulsed flow, and used helium bubbles and high speed digital photography to obtain an insight into the flow structure of the generated downburst (Mason, *et al*. 2005). The influence of jet inclination for both steady and rapidly accelerated jet flows was investigated by Mason and Wood (2005). In this instance the flow acceleration was produced by stretching a thin latex membrane across a support board positioned downstream of the nozzle. Using a different technique, Hoxey, *et al*. (2003) outlined an impinging jet arrangement installed into the former Silsoe Research Institute Atmospheric Flow Laboratory, to study the behaviour of the downdraft both in still air and in a cross flow. In this instance the downburst was generated by manually opening and closing a flap which diverted air into the impinging jet. Flow visualisation results carried out under cross flow conditions provided evidence of a ring vortex being formed that restricts the downburst from expanding into the oncoming wind. In addition to the above there has been a variety of simulations, mainly at a small scale, which have examined physically a variety of impinging jets. The results obtained from these experiments have been used mainly to validate CFD simulations (see for example Kim and Hangan 2007). The benefit of adopting such a computational approach enables the issue of up-scaling to be addressed.

2.2. Slot jet simulations

One of the main drawbacks with the above physical simulations relates to the scale of experiments, i.e. all of the impinging jets are relatively small when compared to an actual downdraft. In order to address this issue and provide an alternative technique to that of an impinging jet, Lin and Savory (2006) argued that the radial outflow from the downburst can be treated separately to that of the vertical flow associated with the downdraft column. Hence, by treating

these two areas separately it is possible to model physically the outflow in isolation from the downdraft. In order to achieve this in a traditional atmospheric boundary layer (ABL) wind tunnel, an additional source of wind was introduced via a slot at the base of the wind tunnel. When a cross flow was present, this created a mixing layer, whose flow properties compared favourably with those of the impinging studies outlined above. In a later study (Lin, *et al*. 2007) additional experiments were undertaken to investigate the transient characteristics of the jet using an automated gate in order to generate the correct flow profiles (no cross flow was present). While this is a novel approach which enables the flow structure to be examined at a larger scale than outlined previously it does however have a number of drawbacks. It is widely acknowledged that downbursts are three dimensional structures and it is somewhat questionable if two dimensional simulations are a reasonable approximation. However, given the scales simulated by Lin and Savory (1:60 - 1:1400) this is not likely to be a significant issue at present. Another issue which needs consideration is related to the transient nature of the flow within a downburst. By the very nature of the simulation, the slot jet approach is not able to simulate the interaction of the downburst at the location where it initially strikes the ground, where there are potentially high gust velocities. Notwithstanding these limitations, slot jet simulations are a novel approach enabling an insight to be gained at larger scales, and also allow small scale topographic and roughness features to be simulated, which can be difficult with downburst simulations.

3. The University of Birmingham downburst simulator

As outlined above, previous simulations of downburst winds have often not been able to capture the entire flow structure of the outflow winds at a scale that would enable them to be useful for obtaining design loads. Hence, it was decided that in an attempt to circumvent a number of these issues, an impinging jet simulator larger than those outlined above would be developed. The following sections outline the design and equipment used for the Birmingham simulations.

3.1. General description

The general principle of the apparatus is based on previous successful modelling attempts using wall jets to simulate downdrafts, whereby buoyancy induced flow is replaced by fan driven flow and is illustrated in Fig. 1. In the current arrangement, nine axial flow fans, each with a cross sectional area of 0.85 m^2, are used to create the downdraft. Immediately below the fans a honeycomb grid of dimensions 10mm by 10mm with a thickness 100mm was placed in order to

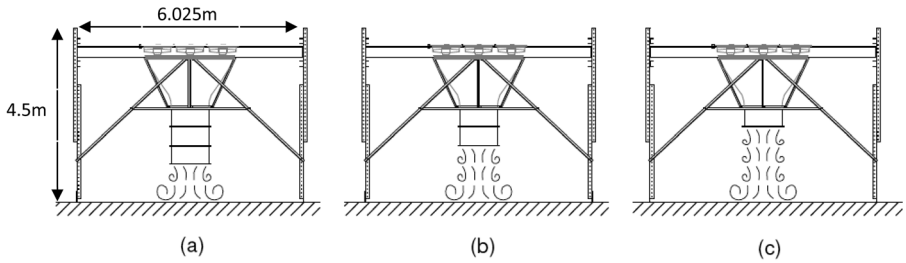

Fig. 1 Schematic of the apparatus used at Birmingham illustrating the three possible nozzle height arrangements: (a) nozzle height = 1.0D; (b) nozzle height = 1.5D; (c) nozzle height = 2.0D, where D is the initial diameter of the jet

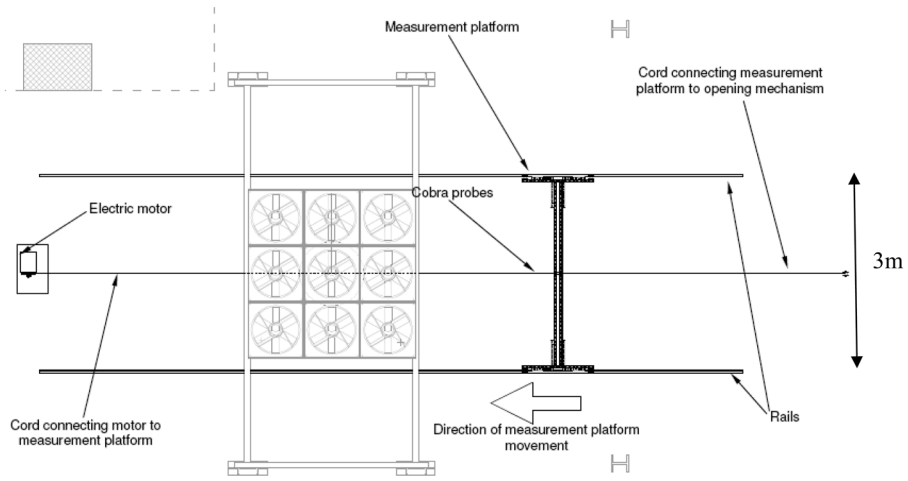

Fig. 2 Plan view of the test apparatus illustrating measurement platform used in the translation tests

reduce swirl. A transition section immediately downstream of the honeycomb channelled the flow from a square cross section to a circular cross section of diameter (D) 1 m. This diameter will be shown later to represent a length scale of around 1:700 and 1:1000 and is adaptable to allow three different nozzle heights H (i.e. the distance between the ground and the end of the nozzle) of 1 m, 1.5 m and 2 m (Fig. 1). The apparatus is capable of producing a mean jet velocity, V_j, of between 6 and 16 ms^{-1} as measured half a diameter below the centre of the nozzle. The turbulence intensity (defined as the standard deviation of the velocity over the mean velocity) measured at the same location for a constant down flow is approximately 15%. Both mean velocities and turbulence intensities were reasonably constant over the width of the jet. For example, at a measurement height of 1.5H, the mean velocity of the jet measured at difference radial distances from the centreline of the jet agreed to within 4%. Similar measurements indicated that the turbulence intensities over the same region were consistent to within 5% (see McConville (2008) for details). Hence, in what follows the centreline of the downdraft is assumed to correspond to the axis of symmetry of the cylindrical nozzle. The apparatus was specifically designed to enable the effect of impingement height to be examined by removing one or more of the flow sections of the nozzle. The large scale of the apparatus meant that moving the fans in order to simulate the translational motion of a thunderstorm was not an option. In order to circumvent this drawback and provide an insight into the effect of such motion, a moveable platform was constructed which when driven by an electric motor passed underneath the downburst simulator at a translational speed (U_t) of 3 ms^{-1} on rails situated 3 m apart and 8 m long (Fig. 2). It should be noted at the outset that the platform only enables the velocity measurement equipment (cobra probes, see section 3.3) to be moved under the downburst, i.e. it is not yet capable of simulating an entire moving ground plane but is useful in terms of providing an insight into transient effects. For a full description of the apparatus and a discussion on issues relating to its design, the reader is referred to McConville (2008).

3.2. Opening mechanisms

Of particular interest is the transient motion of the gust front as it moves outwards. Preparatory

work in this area revealed that the velocity time-history recorded at any given location, in particular the timing and magnitude of the peak velocities associated with the primary radial vortex, depend greatly upon the method of flow acceleration. In order to investigate this issue further it was decided that three different methods of flow acceleration would be used:

- Acceleration of the flow by directly controlling the rotational speed of the fans, ("Fan control").
- Acceleration through use of a mechanism which opened in the plane perpendicular to axis of the jet, ("Sheet control").
- Acceleration through use of a mechanism which opened in the direction of the jet, ("Flap control").

These three opening mechanisms are briefly described below.

Fan control

During the conceptual stage of this project it was envisaged that each fan would have the ability to be controlled independently and the downdraft would be generated by directly controlling the rotational speed of the fans. This method has proved successful in the past in boundary layer simulations (Sterling, *et al*. 2003). To this end the fans were connected to a series of frequency inverters and bespoke software was written to enable communication with the inverters. The response time of the fans, i.e. the time taken for the fans to start from rest and reach a maximum value was of the order of 3 seconds.

Sheet control

Initially it had been anticipated that it would be possible to construct a camera-style aperture, as developed by Mason, *et al*. (2005). However, problems were encountered sourcing the correct materials that were both light weight and strong enough to support the force of the downdraft at the velocities (~16 ms^{-1}) and required size of the sheets (~2 m) used in this study. Ultimately it was decided that it would not be possible to pursue this method of flow acceleration, and a simpler design was needed. To this end, two sheets of plywood were supported on rollers in the horizontal plane, 100 mm below the nozzle. Weights were then applied via a series of pulleys so that once a catch was released the sheets would move apart from one another in the horizontal plane. A 'V' notch was cut into both sheets so that as the jet passed through the plane of the sheets it spread out from the centre. While it is acknowledged that such a system may introduce a degree of asymmetry into the downburst, subsequent analysis has revealed that this asymmetry is within the run-to-run variations experienced using the other two methods.

Flap control

In this approach eight triangular flaps were hinged 100 mm below the nozzle, and pinned together, after which the desired speed of the fans (jet) was set. Once the flow from the nozzle was established the fixing mechanism holding the centre of the flaps in place was released. The force exerted by the jet combined with gravity caused the flaps to rotate around their hinges, enabling the jet to impinge on the floor. The speed at which the flaps open is a consequence of the force applied by the jet, which is of course dependent upon V_j. The flap control mechanism is shown in Fig. 3.

3.3. Measurement equipment

All of the velocity data reported in the current paper were measured using a Series 100 cobra

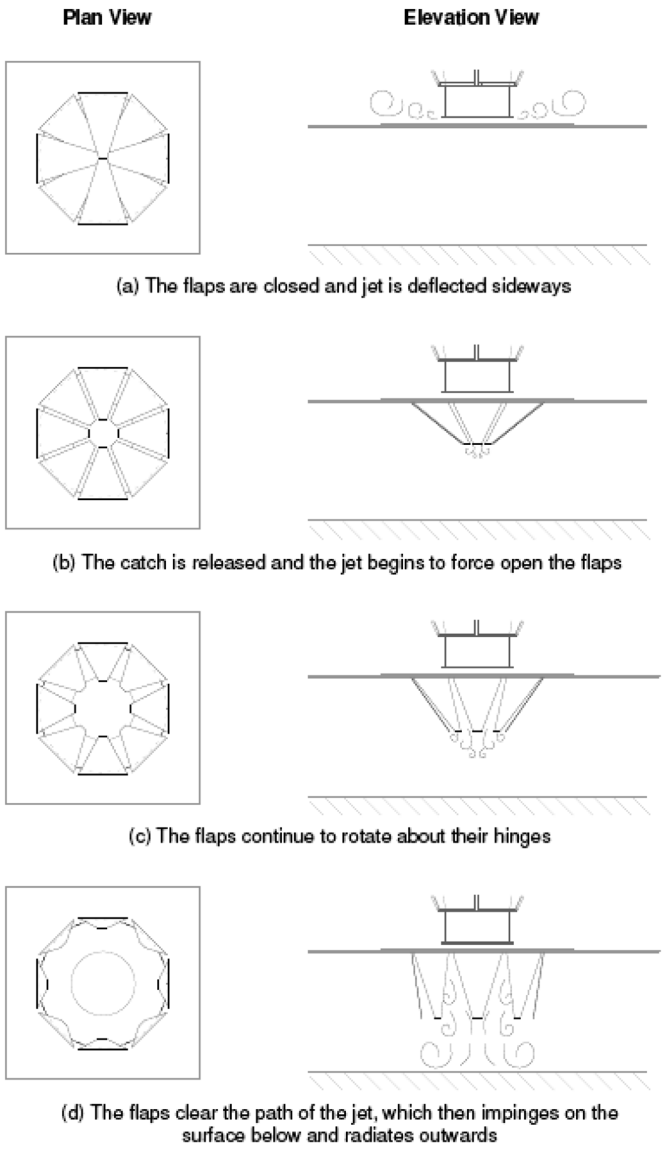

Fig. 3 An illustration depicting plan and elevation views at four stages (a-d) of flow acceleration using the flap control

probe (Turbulent Flow Instrumentation) and sampled at 2500 Hz. The cobra probe is capable of measuring within a cone of range ±45° with an accuracy of approximately ±1° for both pitch and yaw angles. The accuracy of the probe as stated by the manufacturers is of the order of ±0.2 ms^{-1} for velocities in the range 2 - 30 ms^{-1}. An independent check undertaken in a low turbulence wind tunnel supported this claim. Whilst the magnitude of the mean velocity for the experiments reported in the following sections was found to vary, typical values were in the region of 10 ms^{-1}, suggesting that the measured velocity data are on average ±2% of their true values.

Radial distances from the centre of the impingement zone were measured using steel rulers

(accuracy ±1mm representing a percentage error of ±0.04%). Vertical distance measurements were undertaken with steel rulers to which Vernier gauges were fitted, enabling measurements of the order of ±0.1mm to be made. The majority of the data presented below were measured at vertical distances of approximately 20mm above the ground, resulting in a percentage error of the order of 0.5%.

3.4. Ensemble averaging

It was observed early in the experimental programme that, whilst the measured velocities were well defined when a mean flow was established, there was significant run-to-run variation of the experimental results for the developing flow field around the gust front, resulting from the large turbulence scales generated in the flow field. Thus, unless indicated otherwise, results presented below that describe the transient effects are presented as "ensemble averages", where 10 time histories for any particular measurement case are aligned and the results averaged at each time to give an ensemble mean and an ensemble standard deviation. In order to enable comparison between the different datasets, the time is assumed to be zero when the velocity corresponds to 40% of the peak velocity, although this must be regarded as an arbitrary definition.

3.5. Preliminary experiments

Constant outflow velocity

A series of preliminary experiments was undertaken for a constant outflow velocity to investigate the nature of the velocity field within the downdraft and the effect of nozzle height above the ground plane. Normalised velocity profiles are shown in Fig. 4, with the notation adopted for the normalization shown in Fig. 4a. Fig. 4b illustrates the results of the normalised streamwise velocity profiles obtained at various normalized distances (X/D) from the stagnation point for a nozzle height of 2D. In Fig. 4b the vertical axis represents the vertical height (Y) above the ground normalized by the height corresponding to half of the streamwise maximum velocity ($Y_{m/2}$). This normalization is common in terms of representing the flow field associated with a wall jet (see Wygnanski, *et al*. 1992). Also shown in Fig. 4b is the empirical function of Wood, *et al*. (2001) illustrating agreement of the current data with previous studies for values of $Y/Y_{m/2} > 0.2$. It is also

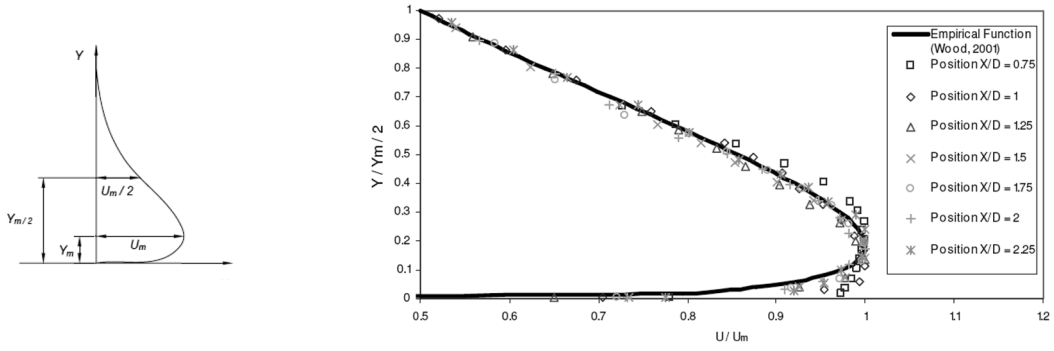

(a) Normalization notation. (b) Experimental data.

Fig. 4 Normalised streamwise velocity profiles under steady state conditions, H/D = 2.0

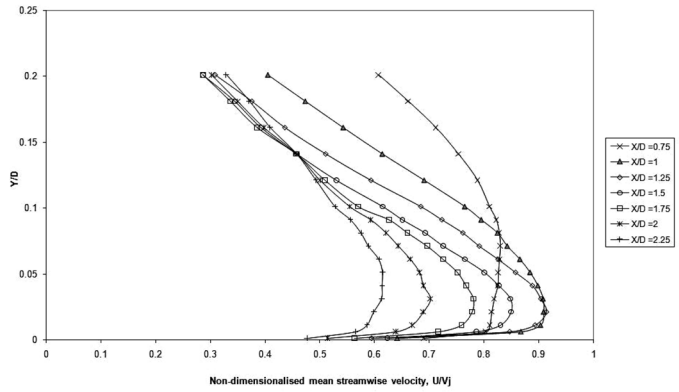

(a) Nozzle Height = 2.0D

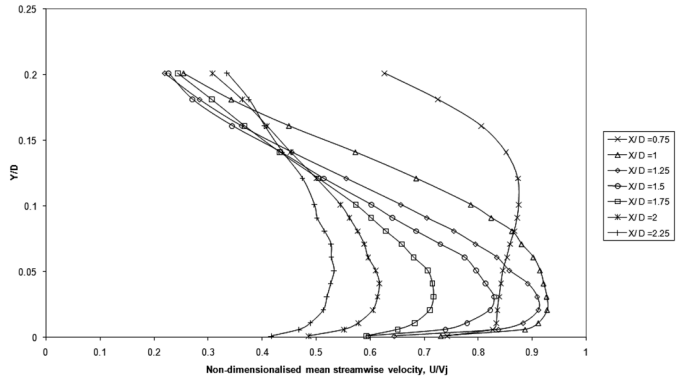

(b) Nozzle height = 1.0D

Fig. 5 Non-dimensionalised steady state velocities for different nozzle heights

evident that for X/D ≥ 1.25 there appears to be a trend towards a full developed wall jet profile.

Fig. 5 shows the time averaged mean velocity profiles for two nozzle heights of H = 2.0D and H = 1.0D, where D is the jet diameter. In general, for values of X/D > 0.75 the profiles have a similar shape, i.e. the height at which the peak in velocity occurs above the ground increases as X/D increases. For values of X/D = 0.75, the mean velocity profile illustrates unusual behaviour and suggests an approximately uniform velocity distribution extending over values of $0 < Y/D < 0.1$.

Flow visualisation

Fig. 6 shows the results of simple flow visualisation experiments using the "fan control" method of simulation. In these experiments, small polystyrene balls (diameter ~4mm) were released from a dispenser located on the edge of the nozzle from which the jet issued. As the fans gather speed, the air flow inside the nozzle and contraction is accelerated and a lower pressure region forms at the edge of the nozzle. Consequently the surrounding air and polystyrene balls are entrained in the jet (Fig. 6b). As the vortex travels towards the ground, further air is entrained, gradually increasing the size of the vortex (Fig. 6c) until it impacts on the ground where it appears to flatten or squash (Fig. 6d), resulting in the flow beneath its core being accelerated. In addition to the balls being released from the dispenser, additional balls were placed along the ground in order to aid with the

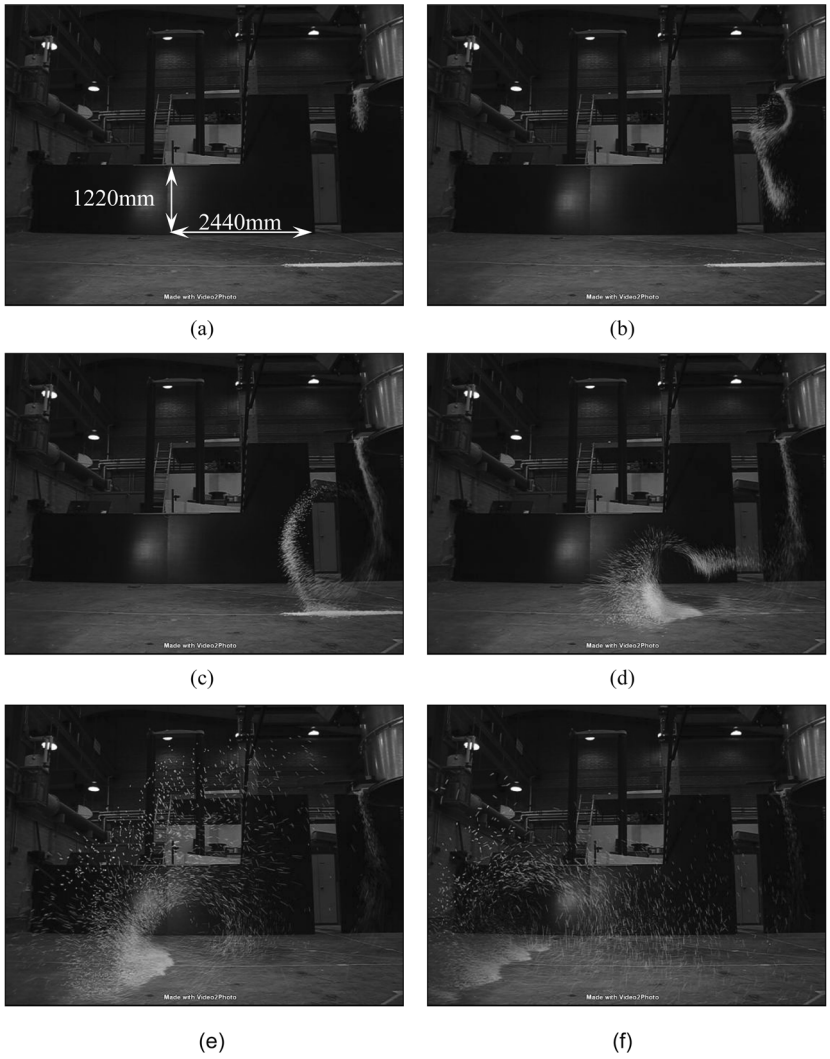

Fig. 6 Flow visualization while accelerating the fans from stationary. (Pictures were taken at intervals of 0.5 seconds and the mean jet velocity = 12.6ms^{-1})

visualisation process. Upon impact the vortex is reduced in size and appears to increase in intensity, especially the flow immediately below the vortex core. In this region it appears that the flow is moving much faster than the flow above the core (Fig. 6e). As the vortex moves away from the point of impact air is again entrained increasing the size, and reducing the intensity (Fig. 6f). Fig. 6f also appears to indicate the non uniform nature of the gust front as it moves along the ground. Similar results were also observed for the sheet control mechanism but for the purposes of brevity are not illustrated. Given the nature of the flaps control mechanism it was not possible to perform such flow visualization experiments since movement of the flaps would interfere with the movement of polystyrene balls. However, interrogation of the velocity data suggests that a similar profile was generated.

It can thus be concluded from these preliminary experiments that the fully developed jet has the

form that would be expected and that the generator can reproduce an axial flow vortex pattern in the start-up phase.

4. Experimental results

4.1. Comparison of different opening mechanisms

Fig. 7 illustrates the velocity time-history corresponding to a location of X/D = 1.25, Y/D = 0.02 and H/D = 2.0, for the three different opening mechanisms. (H is the impingement height, i.e. the distance between the nozzle and the ground). The data in this figure correspond to an ensemble average of ten runs. The local velocity has been normalised by jet reference velocity, V_j which is measured on the centreline of the nozzle, 0.5D below the nozzle and the time has been normalized by the mean jet velocity and downdraft diameter (i.e. $t^* = tV_j/D$). For the case of the fan control mechanism, this was taken to be the value of V_j when the fans had reached a constant rotational speed.

It can be seen that the results for the three opening mechanisms differ considerably. The fan control results and the sheet opening results are dependent upon the nozzle velocity, even when expressed in a non-dimensional form. In particular the peak values for the fan control and the initial rate of increase for the sheet control demonstrate this dependency. Both of these control mechanisms

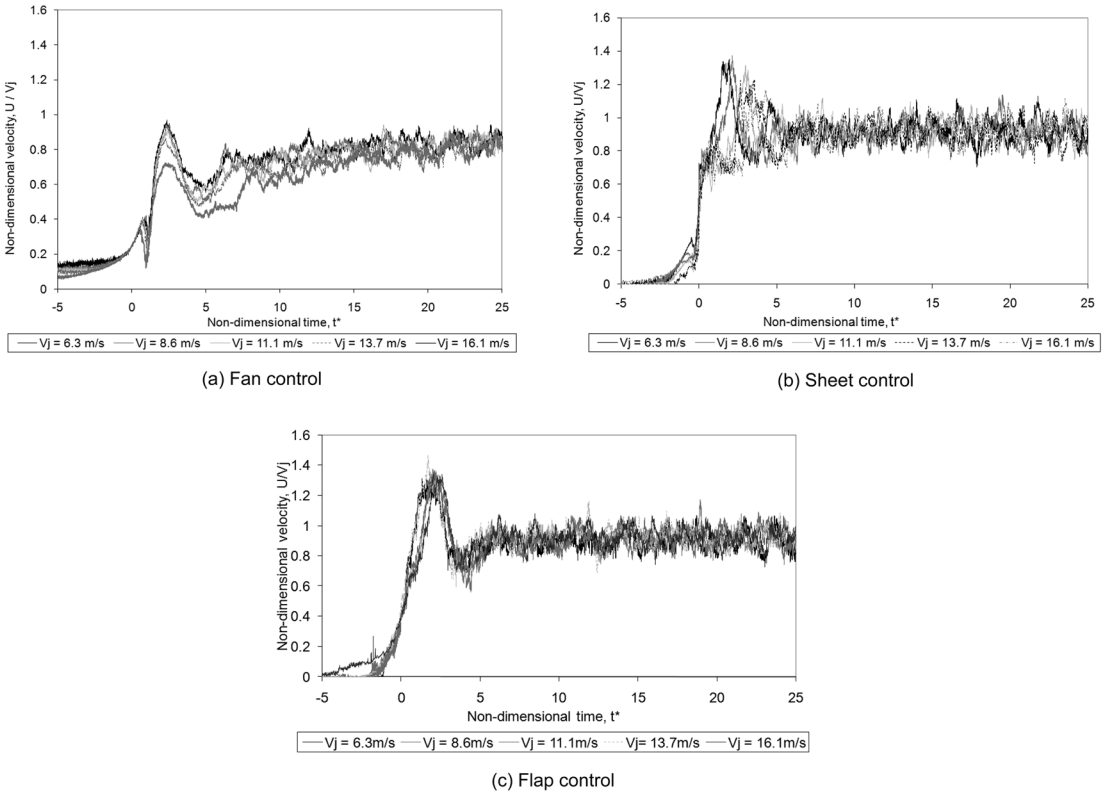

Fig. 7 Non-dimensional velocity versus non-dimensional time, X/D = 1.25, Y/D = 0.02, H/D = 2.0, 10 run ensemble average

also show peaks / plateaus in the initial velocity rise to the peak. By contrast the flap control mechanism is independent of nozzle velocity when plotted in a dimensionless form. All three opening mechanisms give the same steady state conditions, although these are more rapidly approached by the sheet and flap controls than by the direct control.

Based on these results, it would appear that the "flaps control" mechanism is the most suitable, in that the results appear to be independent of nozzle velocity, and it will be shown in section 5 that, through a suitable choice of scaling parameters, the results fit the full-scale data adequately. Thus in what follows, all the results that will be presented were obtained with this opening mechanism.

4.2. Gust front development with radial distance

Fig. 8 illustrates the normalised velocity time series with respect to non-dimensional time for a probe positioned at a variety of radial distances from the centre of the impingement zone. The results in Fig. 8 correspond to a jet velocity (V_j) of 16.1 ms^{-1} and a measurement height of Y/D = 0.021 and H/D = 2.0. It is evident from Fig. 8 that for values of $0.75 \le X/D \le 1.5$, the maximum value of the normalised velocity increases with respect to radial distance. As would be expected the time taken to reach this maximum value is also a function of distance, i.e. the further away from the impingement zone, the longer it takes to reach the maximum value. However, the initial acceleration of the flow appears to be constant for all values of X/D, supporting the idea of a well defined gust structure which changes in intensity as it moves away from the impingement zone.

4.3. Translational simulations

Downbursts are not always stationary events and retain a significant percentage of the parent storms momentum. Translation speeds have been stated to be as high as 30% that of the downdraft velocity (Letchford and Chay 2002) and a number of recent studies have attempted to simulate the moving characteristics of downbursts. One of the drawbacks with the method of downburst simulation used here is the inability to move the fans. However, by changing the frame of reference and moving the ground plane it is possible to achieve a similar effect. The movable platform outlined in section 3.1 was used in conjunction with the 'flap control' acceleration method. The

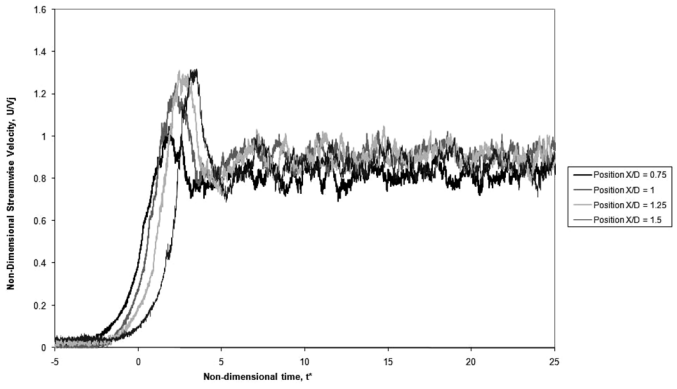

Fig. 8 Non-dimensional velocity time series for increasing radial distances using "flap control" opening. Y/D = 0.021, H/D = 2.0, $V_j = 16.13 ms^{-1}$

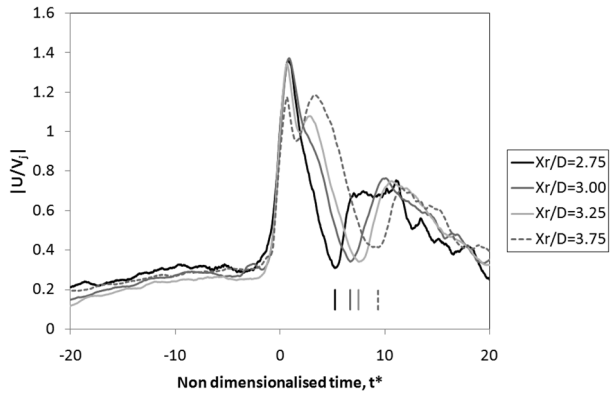

Fig. 9 A 50 point moving ensemble average velocity time series corresponding to the translation simulations. The vertical lines between $5 < t^* < 10$ indicate the regions used by the different probes

velocity of the downdraft (V_j) was set to 11.1 ms^{-1} corresponding to a ratio of the translational speed (U_t) to the jet speed (V_j) of 0.27, and so similar to the translational speeds outlined above. Two cobra probes were mounted on the platform at a height of 15 mm above the ground and were positioned back to back so that one probe recorded data on approach to the downburst, while the other, which was rotated through 180 degrees from the first, recorded data as the platform moved away from the downburst. The distance between the two faces of the cobra probes was 15mm. As the platform accelerated towards the downburst simulator a direct connection between the platform and the flap release mechanism ensured that the probes were at the same radial distance when the downdraft was initiated. By varying the length of this connection it was possible to adjust the position of the platform relative to the centreline of the jet at the start of the simulation i.e. when the flaps were released. Four different radial release distances were investigated, X_r/D = 2.75, 3.00, 3.25 and 3.75. The notation X_r is used to distinguish the current measurements from those presented previously which were recorded at a constant location. It needs to be again emphasized that this is not a full moving ground plane simulation, as only the probes rather than the ground plane were moved. The results are shown in non-dimensional form in Fig. 9 and in order to ease interpretation represent a fifty point running average of the ensemble data. It is perhaps also worth clarifying that this figure represents a snapshot of the results, i.e. data acquisition was started before the flaps were released and the probes were stationary. It is evident from this figure that the shape of the normalised velocity time series is dependent on the radial release distance of the probe when the flaps are opened. At X_r/D = 2.75 a single peak in the time history illustrates that the downburst has just enough time to reach surface level and radiate outwards before the probes pass through the gust front. At X_r/D = 3.00 a local maximum can be observed following the primary peak, and at radial distances of X_r/D greater than 3.00, this local maximum can be seen to grow into the secondary peak as steady flow conditions have time to develop. In constructing Fig. 9 the maximum velocity from either the forward facing or rear facing probe is used. The vertical lines indicated on Fig. 9 illustrate the regions used by the different probes, (to the left of the line is the forward facing probe and to the right is the rear facing probe).

4.4. Variability of results

In some respect the normalisation of the data presented above and time averaged vertical profile

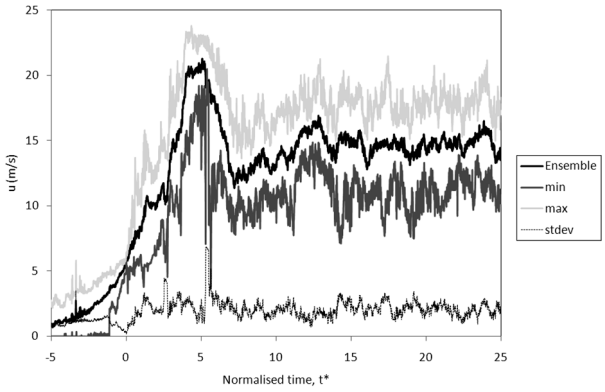

Fig. 10 Ten test ensemble average, X/D = 1.25, Y/D = 0.021, H/D = 2 using 'flaps control' method

of streamwised velocity can be misleading. These two features suggest a well behaved vortex structure whose features can readily be predicted. However, all of the results presented above relate to a 10 run ensemble averaged data set and no attempt has been made to explore the variability of individual simulations. Fig. 10 illustrates the velocity time series obtained from a 10 test ensemble average, corresponding to a non moving simulation. In this figure, the solid black line indicates the ensemble average, which highlights the features observed previously. Also shown are the maximum and minimum velocities obtained at each time step across the entire 10 runs, i.e. the data corresponding to the maximum and minimum envelopes. The value of peak gust can be seen to vary in the range 24 ms^{-1} - 19 ms^{-1}. Also worth noting are the number of successive peaks in the 'maximum' data which occur around the peak gust. Fig. 10 also shows the ensemble standard deviation, which illustrates that after the passage of the peak gust, the flow is reasonably statistically 'stationary'. For steady state conditions the average turbulence intensity (standard deviation / mean) is approximately 20%.

5. Scaling and comparison with full scale data

5.1. The issue of scale

A problem that has to be faced when comparing any physical simulation with reality is that of determining the relevant scales. The following relationship is often assumed:

$$r_V = \frac{r_L}{r_T} \tag{1}$$

where r_V is the ratio of full-scale to model-scale characteristic velocity, r_L is the ratio of the full-scale to model-scale characteristic length, and r_T is the ratio of the full-scale to model-scale characteristic time. It is obvious that if any of these two scales are specified then the third scale is automatically given by Eq. (1). The velocity scale is relatively straightforward to specify, i.e. r_V = maximum horizontal outflow velocity at full-scale / maximum horizontal outflow velocity corresponding to the simulated downburst. There are a number of possible ways of determining the ratio r_L, but perhaps the most common, in the study of boundary layer winds, is to ensure that the model scale matches the ratio of full-scale to model scale surface roughness lengths (i.e. z_o). However, for the purposes

of the current paper, specifying the equivalent roughness lengths is not possible since the velocity profile cannot be represented by a log-law. An alternative way might be to determine the scale ratio from the ratio of full-scale to model scale turbulence length scales. Again, given the lack of full-scale data and the non-stationarity of a downburst, this is not straightforward. Another possible way in which to obtain r_L is to calculate the ratio between the downdraft diameter and that of the nozzle diameter. There are of course a number of issues associated with such an approach. Firstly, such a procedure assumes that the full-scale downdraft is circular and secondly, information pertaining to the diameter of the downdraft is known. While it is not unreasonable to assume that such an estimate can be made of this parameter, the consequence is that such an approach will only ever yield approximate values. Another possible approach to obtaining r_L is to assume implicitly that the simulation is correct and to interrogate the normalized velocity time series obtained at various heights above the ground and to compare them to full-scale data measurements. Once the best agreement is found, r_L is then given by the ratio of the height at which the full-scale velocity data were obtained to that of the height at which the best fit simulated velocity measurements were obtained.

In what follows we will for the purposes of simplicity obtain the velocity scale by matching the peak full-scale and peak simulated values. We will then compare the normalized velocity time series for a variety of radial release positions in order to achieve a suitable match. This will then enable the full-scale value of the downdraft diameter to be calculated and compared with existing estimates.

5.2. Comparisons with full-scale data

Data obtained from the 'flaps' simulation were used to compare with data recorded at full-scale. However, unlike the above analysis, data from individual runs were used rather than ensemble averages since the full-scale data correspond to an individual event and not an ensemble of events.

A comparison was made with full-scale data recorded at Andrews Air Force Base near Washington D.C. on August 1st 1983 (Fujita 1985). The data were recorded using a propeller anemometer at a height of 4.9 m above the ground. Previous studies (Letchford and Chay 2002) have reported that the translational speed of the storm was estimated at 25 kts (~ 13 ms^{-1}). Estimates of the diameter of the downdraft vary from an initial 700 m (Holmes and Oliver 2000) up to 1000 m, increasing at a rate of 30 m per minute (Chay and Albermani 2000; Chay, *et al*. 2006). It has been reported that peak horizontal winds reached 67 ms^{-1}. For a worst case scenario, the results in Fig. 7 suggest that a ratio of the order of 1.3 between the peak wind speed and downdraft jet speed is not an unreasonable assumption. However, it should be noted that Fig. 7 is for an ensemble average of 10 runs and as stated above comparisons should be made with individual runs and not ensemble events. The run found to give the best agreement between the simulated and full-scale data resulted in a ratio of 1.5. Hence, the full-scale equivalent of V_j is estimated to be of the order of 44 ms^{-1}, which when combined with the translational speed of the storm, gives a translational ratio (V_j/U_t) of approximately 0.3. This result is compared with the results of moving simulations for this translational ratio in Fig. 11, for a simulation jet velocity of 11.1ms^{-1} i.e. r_V~4.0. The full scale value of the jet diameter that gave the best fit to the simulated values was then found. This procedure was repeated for a number of different locations as illustrated in Fig. 11. The results for the simulations are illustrated for a single physical simulation as opposed to an ensemble average. In Fig. 11 it should be noted that the experimental values of D and Vj have been used to obtain t* for the experimental data whereas the assumed full-scale equivalent values have been used to obtain t* for

the full-scale data. Table 1 illustrates the full-scale downdraft diameter corresponding to the radial position at release.

Generally, Fig. 11 illustrates reasonably good agreement between the simulated and full-scale data. However, these results and the corresponding estimation of scale must be interpreted with caution. As stated previously only the probes are moving during these simulations (i.e. the jet and the ground surface are stationary). This results in conditions which are not necessarily typical of those which occur

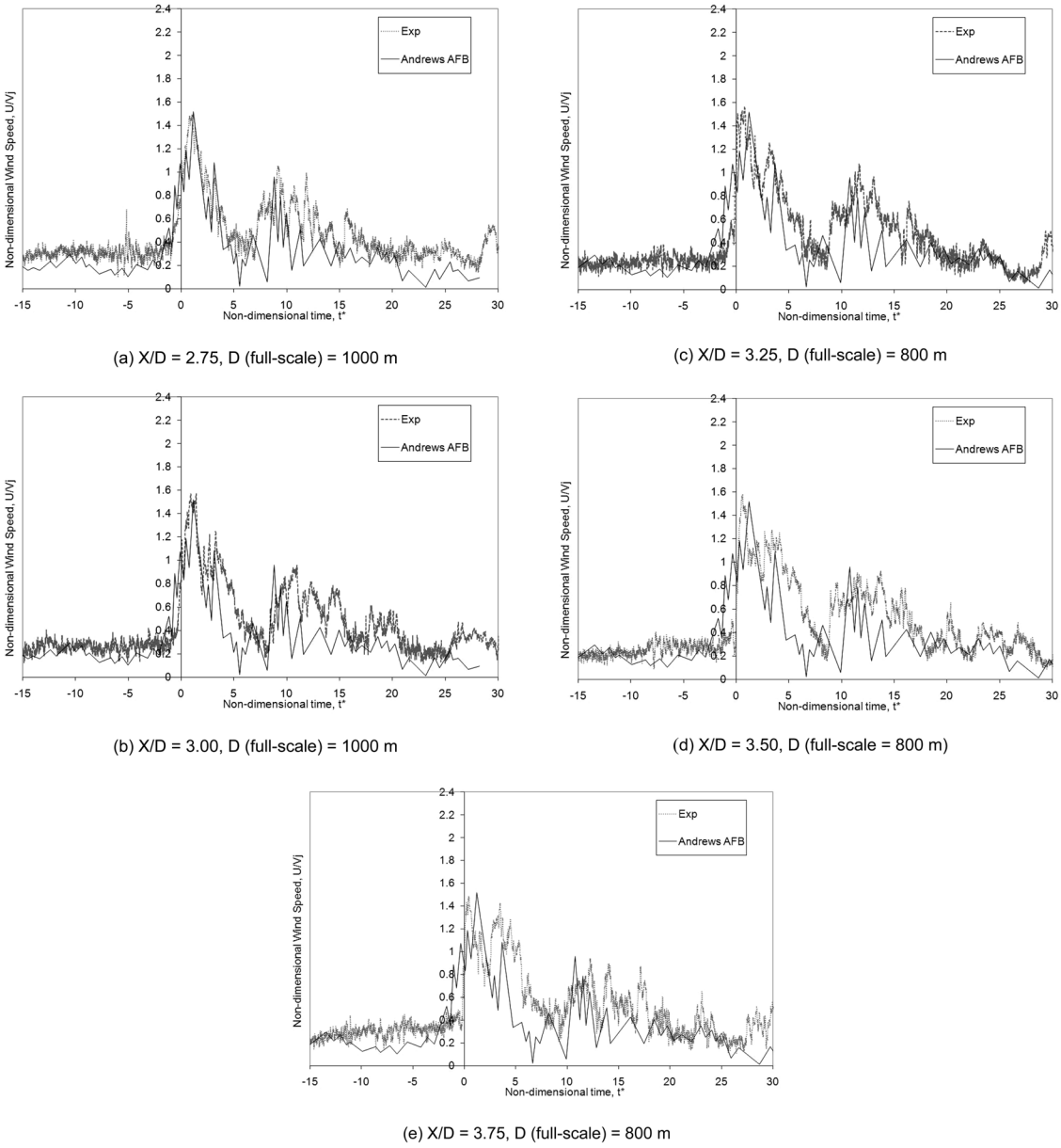

Fig. 11 Non-dimensional simulated velocity data, and full-scale velocity data corresponding to the Andrews AFB event

Table 1 Estimated full-scale downdraft diameter for varying radial distances

Radial position at release (X/D)	Full-scale D (m)
2.75	1000
3.00	1000
3.25	800
3.50	800
3.75	800

in reality. Also, the moving simulations relate to data recorded at 15mm above the ground. There is the possibility that other heights might also yield good agreements between the measured and the full-scale data. If this were the case, then the estimates of scale given in Table 1 would undoubtedly change. There is also the issue of the difference in surface roughness between the full-scale data and that of the experimental conditions. However, it could be argued that the effect of the latter is small in comparison with aforementioned assumptions. Nevertheless, this simple technique illustrates remarkable promise.

6. Conclusions

This paper has examined the feasibility of using a relatively large scale simulator in order to generate conditions which may occur as a result of a thunderstorm downburst. The main conclusions are:

- The mean velocity profiles recorded during steady state conditions are in agreement with previous studies and empirical relationships, e.g. Wood, *et al*. (2001).
- For values of X/D the mean velocity profile is shown to be a function of distance from the centre of the impingement zone and nozzle height (Fig. 5).
- Within the downdraft velocity range tested, the flap control mechanism was shown to be independent of downdraft velocity, whereas the other two mechanisms illustrate some degree of dependency (Fig. 7).
- For all control methods examined there appears to be a well defined gust structure. The results of Fig. 8 illustrate a reasonably constant increase in velocity for a variety of distances from the centre of the impingement zone was observed.
- A significant degree of run-to-run variability was observed during each experiment.
- The issue of scaling is not straightforward and open to interpretation. However, a visual comparison of the current simulations with that of the full-scale event illustrates a favourable comparison.

Acknowledgements

The authors would like to thank the Royal Society whose funding enabled the construction of the downburst simulator and also Mr. M. Vanderstam of the University of Birmingham who undertook the construction.

References

Byers, H.R. (1959), *General Meteorology*, 3rd edition, McGraw-Hill, New York.
Chay, M.T., Albermani, F. and Wilson, R. (2006), "Numerical and analytical simulation of downdraft wind

loads", *Eng. Struct.*, **28**(2), 240-254.
Chay, M.T. and Albermani, F. (2000), "Dynamic response of a SDOF system subjected to a simulated downdraft", *Proc. of 6th Asia-Pacific Conf. on Wind Engineering (APCWE-VI)*, Seoul, Korea, 12-14 September 2005, 1562-1584.
Chay, M.T. and Letchford, C.W. (2002), "Pressure distributions on a cube in a simulated thunderstorm downdraft, Part A: stationary downdraft observations", *J. Wind Eng. Ind. Aerod.*, **90**(7), 711-732.
Durañona, V., Sterling, M. and Baker, C.J. (2006), "An analysis of extreme non-synoptic winds", *J. Wind Eng. Ind. Aerod.*, **95**, 1007-1027.
Fujita, T.T. (1985), "The Downburst", *Reports of Projects NIMROD and JAWS*, University of Chicago.
Holmes, J.D. (1992), "Physical modelling of thunderstorm downdrafts by wind tunnel jet", *Second AWES Workshop*, Healesville, Victoria, 29-32.
Holmes, J.D. and Oliver, S.E. (2000), "An empirical model of a downdraft", *Eng. Struct.*, **22**(9), 638-645.
Holmes, J.D., Hangan, H.M., Schroeder, J.L., Letchford, C.W. and Orwig, K.D. (2008), "A forensic study of the Lubbock-Reese downdraft of 2002", *Wind Struct.*, **11**, 137-152.
Hoxey, R.P., Robertson, A., Toy, N., Parke, G.A.R. and Disney, P. (2003), "Design of an experimental arrangement to study wind loads on transmission towers due to downdrafts", *Proc. of 2nd Int. Conf. on Fluid Structure Interaction*, Cadiz, Spain, 24-26 June 2003, 395-404.
Kim, J. and Hangan, H. (2007), "Numerical simulations of impinging jets with application to downdrafts", *J. Wind Eng. Ind. Aerod.*, **95**, 279-298.
Letchford, C.W. and Chay, M.T. (2002), "Pressure distributions on a cube in a simulated thunderstorm downdraft, Part B: moving downdraft observations", *J. Wind Eng. Ind. Aerod.*, **90**(7), 733-753.
Letchford, C.W., Mans, C. and Chay, M.T. (2002), "Thunderstorms—their importance in wind engineering (a case for the next generation wind tunnel)", *J. Wind Eng. Ind. Aerod.*, **90**(12-15), 1415-1433.
Lin, W.E. and Savory, E. (2006), "Large-scale quasi-steady modelling of a downdraft outflow using a slot jet", *Wind Struct.*, **9**(6), 419-440.
Lin, W.E., Orf, L.G., Savory, E. and Novacco, C. (2007), "Proposed large-scale modelling of the transient features of a downdraft outflow", *Wind Struct.*, **10**(4), 315-346.
Mason, M. and Wood, G. (2005), "Influence of jet inclination on structural loading in an experimentally simulated microburst", *6th Asia-Pacific Conf. on Wind Engineering (APCWE-VI)*, Seoul, Korea, 12-14 September 2005, 2758-2770.
Mason, M., Letchford, C. W. and James, D.L. (2005), "Pulsed wall jet simulation of a stationary thunderstorm downdraft, Part A: Physical structure and flow field characterization", *J. Wind Eng. Ind. Aerod.*, **93**(7), 557-580.
McConville, A.C. (2008), "Physical simulation of thunderstorm downdrafts", PhD thesis, University of Birmingham, UK.
Sterling, M., Baker, C.J., Berry, P.M. and Wade, A. (2003), "An experimental investigation of the lodging of wheat", *Agr. Forest Meteorol.*, **119**(3-4), 149-165.
Wakimoto, R.M. (1982), "The life cycle of a thunderstorm gust front as viewed with Doppler radar and rawinsonde data", *Monthly Weather Review*, **110**, 1060-1082.
Wakimoto, R.M. (2001), "Convectively driven high wind events", *Severe Convective Storms*, *Meteorological Monographs*, **28**, 255-298.
Walker, G.R. (1992), "Wind engineering beyond the boundary layer wind tunnel", *J. Wind Eng. Ind. Aerod.*, **41-43**, 93-104.
Wood, G.S., Kwok, K.C.S., Motteram, N.A. and Fletcher, D.F. (2001), "Physical and numerical modelling of thunderstorm downdrafts", *J. Wind Eng. Ind. Aerod.*, **89**, 535–552.
Wygnanski, I., Katz, Y. and Horev, E. (1992), "On the applicability of various scaling laws to the turbulent wall jet", *J. Fluid Mech.*, **234**, 669-690.

JH